

Gamma-Ray Spectroscopy of Low-Lying Levels in $^{28}\text{Mg}^\dagger$

T. R. Fisher, T. T. Bardin, J. A. Becker, L. F. Chase, Jr., D. Kohler, R. E. McDonald, A. R. Poletti,
and J. G. Pronko

Lockheed Palo Alto Research Laboratory, Palo Alto, California 94304

(Received 19 December 1972)

Excitation energies, spins, and nuclear lifetimes have been measured in ^{28}Mg by employing the reaction $^{26}\text{Mg}(t, p\gamma)^{28}\text{Mg}$ at bombarding energies in the neighborhood of 2.9 MeV. Reaction-produced protons were detected in an annular Si counter at an average angle of 171° , and coincident- γ -ray spectra were obtained with both NaI(Tl) and Ge(Li) detectors at angles $120^\circ \geq \theta \geq 0^\circ$. γ -ray angular distributions were extracted from data obtained with the NaI(Tl) detectors, while precision γ -ray energies and Doppler-shift attenuations were extracted from the data collected with the Ge(Li) detector. The results obtained for excitation energies (keV), spins, and lifetimes (psec) are: 1473.8 ± 0.4 , 2, 1.60 ± 0.20 ; 3862.9 ± 0.7 , 0, 1 or 2, 0.75 ± 0.10 ; 4021.2 ± 1.6 , 4, 0.21 ± 0.07 ; 4557.4 ± 0.8 , 2, < 0.04 ; 4877 ± 4 , 2, < 0.18 ; 5171.6 ± 0.8 , 3, 0.10 ± 0.07 ; 5190.7 ± 3.0 , 1, < 0.03 ; 5470.5 ± 5 , 2, undetermined. γ -ray branching ratios and multipole-mixing ratios were also obtained from the data, and reduced electromagnetic transition matrix elements have been extracted for all transitions observed. The results are compared with the predictions of both the triaxial rotor model of Kurath and the shell-model calculations of de Voigt and Wildenthal.

I. INTRODUCTION

Adequate theoretical calculations of the spectroscopic properties of nuclei in the middle of the s - d shell have only recently become available. Many of these nuclei do not exhibit the rotational spectra characteristic of nuclei to which the Nilsson model has been applied with success, and complete shell-model calculations are formidable because of the size of the configuration space involved. The lack of success of other approaches, however, seems to indicate that extensive shell-model calculations offer the only real hope for an understanding of these nuclei. It has been demonstrated^{1, 2} that such calculations for $A = 24$ - 32 nuclei are possible within a truncated s - d configuration space. Also Kurath³ has extended the rotational model to nuclei in this mass region by adding an additional degree of freedom. It is thus desirable to obtain information on the spectroscopy of these nuclei in order to test these more sophisticated models. The nucleus ^{28}Mg , which is important to this problem, has received little experimental attention thus far. Excitation energies and some J^π values have been determined,⁴ but no information on electromagnetic transition rates was available at the inception of this work and no theoretical calculations had been reported.

This paper presents the results of an experimental study of the spectroscopy of the low-lying levels in ^{28}Mg . Some of the data have been given previously.⁵ The ^{28}Mg levels were populated through the $^{26}\text{Mg}(t, p)^{28}\text{Mg}$ reaction ($Q = +6.46$ MeV), the only reaction by which this nucleus is readily accessible. Accurate determinations of level excita-

tion energies and nuclear lifetimes were made by precision Ge(Li)- γ -ray spectroscopy; level spins, γ -ray multipole-mixing ratios, and γ -ray branching ratios were determined from angular-correlation measurements employing the Method II geometry of Litherland and Ferguson.⁶ The experimental results for excitation energies and electromagnetic transition matrix elements are compared with the predictions of the triaxial rotor model of Kurath³ and with shell-model calculations by de Voigt and Wildenthal.⁷

II. EXPERIMENTAL PROCEDURE

A. General Experimental Approach

Isotopic targets enriched to 99% ^{26}Mg were bombarded by tritons from the Lockheed 3-MV Van de Graaff accelerator. For the measurements of excitation energies, branching ratios, and lifetimes, proton spectra from an annular silicon detector subtending an angle from 167° to 175° were recorded in time coincidence with γ -ray pulses from a 20-cm³ Ge(Li) detector. For the angular-correlation, as well as the γ -ray branching ratio measurements, the proton spectra were recorded in coincidence with the γ -ray pulses from 10×10 -cm NaI(Tl) detectors. A typical proton spectrum obtained with a ^{28}Mg target ($200 \mu\text{g}/\text{cm}^2$ in areal density) is shown in Fig. 1. The pulse-height matrix of time-coincident proton- γ -ray events was recorded by a data collection system which employed conventional modular electronics and a SEL 810A computer interfaced with two 8192- and one 128-channel analog-to-digital converters. Three-parameter data were recorded event by event on mag-

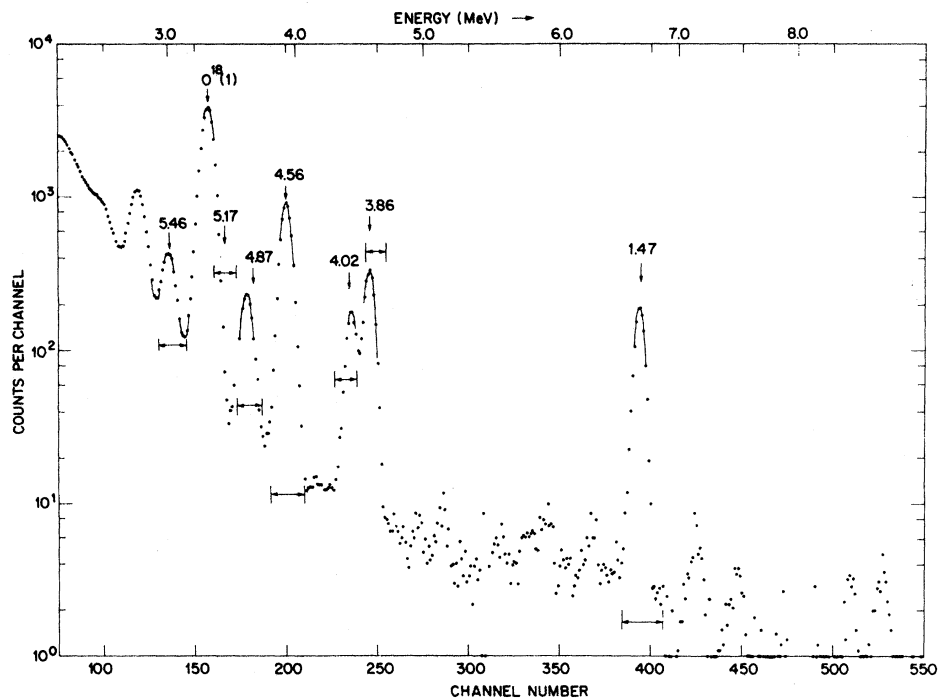


FIG. 1. Proton spectrum in coincidence with all γ rays with $E_\gamma > 1.0$ MeV in the $^{26}\text{Mg}(t, p)^{28}\text{Mg}$ reaction. The thickness of the ^{26}Mg target is $200 \mu\text{g}/\text{cm}^2$. The horizontal arrows indicate the position of the digital windows used in extracting the angular correlations.

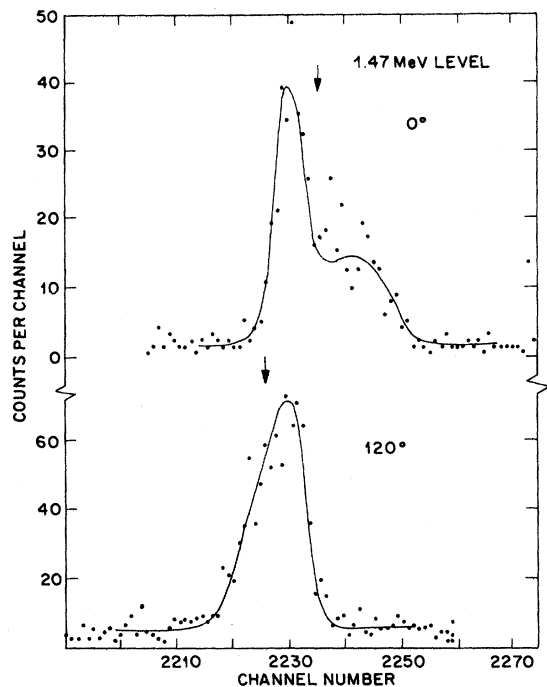


FIG. 2. Attenuated Doppler-shift spectra for the 1.47-MeV γ ray in coincidence with the 1.47-MeV group in the proton spectrum. The curves have been calculated for a lifetime $\tau_m = 1.6$ psec; arrows indicate the centroids of the peaks.

netic tape and subsequently analyzed off line.⁸ The analysis of the γ -ray spectra gated by various proton groups included the subtraction of random coincidences and gain stabilization employing a reference peak [the 1.778-MeV γ ray from $^{28}\text{Al}(\beta^-)^{28}\text{Si}$].

B. γ -Ray Energies, Branching Ratios, and Nuclear Lifetimes

Measurements of γ -ray energies, branching ratios, and lifetimes were performed with a thick ^{26}Mg target ($5.5 \text{ mg}/\text{cm}^2$) at $E_t = 2.9$ MeV. Excitation energies were extracted from the energies of the γ -ray transitions observed in the Ge(Li) spectra with the detector at 90° , 60° , and 120° . In the determination of γ -ray energies, the sources ^{60}Co , ^{228}Th , and ^{28}Al (present as a result of the ^{28}Mg decay) were used to provide γ -ray reference standards. The extrapolation of the energy scale from $2.6 \leq E_\gamma (\text{MeV}) \leq 5$ was checked by comparing the positions of full-energy, one-escape, and two-escape peaks for the high-energy γ rays. Relative γ -ray intensities were translated into branching ratios (or upper limits) after corrections for detector efficiency and angular-distribution effects were applied. The information on γ -ray energies and branching ratios is summarized in Table I. The excitation energies presented in Table I agree

TABLE I. Energies and branching ratios for γ -ray transitions in ^{28}Mg .

E_i (MeV)	E_f (MeV)	γ -ray energy (keV)	Branch (%)	Excitation energy ^a (keV)
1.47	0	1473.8 \pm 0.4	100	1473.8 \pm 0.4
3.86	1.47	2388.9 \pm 0.6	100	3862.9 \pm 0.7
4.02	1.47	2547.2 \pm 1.5	100	4021.2 \pm 1.6
4.56	0		<3	
	1.47	3083.4 \pm 0.7	100	4557.4 \pm 0.8
4.88	0	4877 \pm 10	20 \pm 3	4877 \pm 4
	1.47	3402.5 \pm 4.0	80 \pm 3	
	3.86		<2	
	4.02		<3	
	4.56		<2	
5.17	1.47	3697.5 \pm 0.7	64 \pm 3	5171.6 \pm 0.8
	4.02	1150.3 \pm 0.4	36 \pm 3	
	4.56		<0.5	
	4.88		<5	
5.19	0	5190.2 \pm 3.0	100	5190.7 \pm 3.0
	1.47		<15	
	3.86		<5	
	4.56		<6	
	4.88		<15	
5.47	0		<2	
	1.47	3996.5 \pm 5	100	5470.5 \pm 5

^a Corrections for nuclear recoil have been applied.

well with those quoted by Middleton and Pullen⁴; the γ -ray branching ratios are newly reported.

Nuclear lifetimes were extracted by analyzing the attenuated Doppler shifts measured at γ -ray detector angles of 0, 60, 90, and 120°. As an example, the full-energy peak for the 1.47-MeV γ ray at two different detection angles is shown in Fig. 2. The ^{28}Mg target used was approximately 1.2 MeV thick to the incident triton beam, and the production of ^{28}Mg recoils is cut off by the rapid decrease of the (t, p) cross section below 2 MeV

so that it was not necessary to correct for recoils escaping from the target. To compute the average recoil velocity, the yield as a function of energy for the proton groups populating the various ^{28}Mg levels was deduced from a shape analysis of the thick-target proton spectra in coincidence with various γ rays. This information was translated into an average velocity for the excited ^{28}Mg recoils using the thick-target yield formulas of Baradin.⁹ The information on lifetimes is presented in Table II. The column labeled ΔE_γ is the measured Doppler shift between 0 and 120°, and the column labeled \bar{E}_t gives the average triton bombarding energy from which the full Doppler shift can be calculated.

Values of τ_m have been extracted using the stopping theory of Lindhard, Scharff, and Schiøtt¹⁰ and Blaugrund.¹¹ However, experimental data on electronic stopping cross sections¹² indicate that K_e for Mg may deviate significantly from the Lindhard, Scharff, and Schiøtt estimate; thus the following procedure was used to obtain the value of K_e used in the present analysis. The lifetime of the first excited state of ^{24}Mg ($E_x = 1.368$ MeV) is known very accurately. The average of four recent measurements¹³ employing resonance fluorescence and Coulomb-excitation techniques is $\tau_m = 2.07 \pm 0.07$ psec. This information was used to obtain a measurement of K_e for ^{24}Mg stopping in ^{24}Mg by analyzing the Doppler shifts of the 1.368-MeV γ ray observed when ^{24}Mg is Coulomb excited by 4.5-MeV α particles. The result, $K_e = 2.70 \pm 0.16$ keV cm²/g, is 11% less than the Ref. 10 estimate, in agreement with the general trends reported in Ref. 12. This same 11% reduction was applied to the case of ^{28}Mg stopping in ^{28}Mg resulting in $K_e = 2.54 \pm 0.15$ keV cm²/μg, the value used in the analysis of the present results.

TABLE II. Doppler-shift lifetime measurements in ^{28}Mg . ΔE_γ is the attenuated shift measured between 0 and 120°, and F_m is the ratio of the attenuated shift to the calculated full shift.

E_x (MeV)	Transitions (MeV)	E_γ (keV)	ΔE_γ (keV)	\bar{E}_t ^a (MeV)	F_m	τ_m (psec) ^b
1.47	1.47 \rightarrow 0	1473.8	6.17 \pm 0.50	2.32	0.327 \pm 0.027	1.60 \pm 0.20
3.86	3.86 \rightarrow 1.47	2388.9	14.56 \pm 0.70	2.37	0.520 \pm 0.025	0.75 \pm 0.10
	1.47 \rightarrow 0	1473.8	3.15 \pm 0.80		0.183 \pm 0.046	
4.02	4.02 \rightarrow 1.47	2547.2	24.35 \pm 1.21	2.37	0.816 \pm 0.041	0.21 \pm 0.07
4.56	4.56 \rightarrow 1.47	3083.4	36.29 \pm 1.20	2.50	1.02 \pm 0.04	<0.04 ^c
4.88	4.88 \rightarrow 1.47	3403.0	45.0 \pm 6.0	2.50	1.14 \pm 0.15	<0.18 ^c
5.17	5.17 \rightarrow 1.47	3697.5	36.56 \pm 0.60	2.51	0.896 \pm 0.015	0.10 \pm 0.03
	5.17 \rightarrow 4.02	1150.3	11.52 \pm 0.80		0.897 \pm 0.062	
5.19	5.19 \rightarrow 0	5190.0	59.64 \pm 1.30	2.51	1.03 \pm 0.03	<0.03 ^c

^a \bar{E}_t is the weighted triton energy in the thick ^{28}Mg target calculated from a thick-target yield function.

^b $K_e = 2.54$ keV cm²/μg. Errors in τ_m include a $\pm 10\%$ uncertainty in K_e in addition to statistical uncertainties.

^c Lifetime limits correspond to the 90% confidence level.

TABLE III. Legendre polynomial coefficients for the angular-correlation data obtained with the $^{26}\text{Mg}(t, p\gamma)^{28}\text{Mg}$ reaction. The data have been corrected for the finite solid angle of the γ -ray detectors.

E_x (MeV)	Transition (MeV)	$E_t = 2.5$ MeV		$E_t = 2.9$ MeV	
		A_2/A_0	A_4/A_0	A_2/A_0	A_4/A_0
1.47	1.47 \rightarrow 0	0.63 \pm 0.04	-1.77 \pm 0.07	0.52 \pm 0.03	-0.09 \pm 0.04
3.86	3.86 \rightarrow 1.47	-0.05 \pm 0.04	0.04 \pm 0.04	-0.02 \pm 0.05	0.05 \pm 0.05
	1.47 \rightarrow 0	0.01 \pm 0.04	-0.07 \pm 0.07	0.05 \pm 0.05	0.12 \pm 0.06
4.02	4.02 \rightarrow 1.47			0.48 \pm 0.05	-0.39 \pm 0.07
	1.47 \rightarrow 0			0.56 \pm 0.05	-0.24 \pm 0.07
4.56	4.56 \rightarrow 1.47	0.37 \pm 0.06	-0.14 \pm 0.09	0.43 \pm 0.03	0.09 \pm 0.03
	1.47 \rightarrow 0	0.25 \pm 0.05	0.76 \pm 0.09	0.38 \pm 0.03	0.88 \pm 0.03
4.88	4.88 \rightarrow 1.47	-0.06 \pm 0.08	0.04 \pm 0.13	0.04 \pm 0.06	0.04 \pm 0.07
	1.47 \rightarrow 0	0.48 \pm 0.09	0.72 \pm 0.14		
5.17	4.88 \rightarrow 0			0.40 \pm 0.13	0.05 \pm 0.15
	5.17 \rightarrow 1.47			-0.28 \pm 0.04	-0.05 \pm 0.04
	5.17 \rightarrow 4.02			0.14 \pm 0.06	-0.03 \pm 0.06
5.19	4.02 \rightarrow 1.47			0.47 \pm 0.04	-0.32 \pm 0.05
	5.19 \rightarrow 0			-0.81 \pm 0.04	-0.05 \pm 0.03
5.47	5.47 \rightarrow 1.47			0.43 \pm 0.05	0.04 \pm 0.05
	1.47 \rightarrow 0			0.31 \pm 0.04	0.36 \pm 0.05

C. Proton- γ -Ray Angular Correlations

Two separate measurements of the proton- γ -ray angular correlations were performed. In the first, a target of ^{26}Mg (50 $\mu\text{g}/\text{cm}^2$ in areal density) was prepared by vacuum evaporation onto 10- $\mu\text{g}/\text{cm}^2$ C foils and bombarded by a 2.54-MeV triton beam. γ rays were detected by a single 10-cm \times 10-cm NaI(Tl) detector with its front face 9.5 cm from the reaction site. In the second measurement, a self-supporting foil target (200 $\mu\text{g}/\text{cm}^2$) was bombarded by a 2.9-MeV triton beam and γ rays were

recorded simultaneously in five 10-cm \times 10-cm NaI(Tl) detectors positioned 20 cm from the target at angles of 5, 35, 45, 60, and 90 $^\circ$ to the beam. The angular-correlation data were analyzed by a least-squares fitting procedure, using the formulas for the Method II geometry of Litherland and Ferguson,⁶ to obtain level spins and mixing ratios. Since the lifetimes of the levels involved are of the order of 1 psec or less, the multipolarity of the transitions (unless unusually large enhancements are present) is limited to dipole or quadrupole. The angular correlations can then be expressed in terms of a Legendre polynomial expansion:

$$W(\theta) = A_0 [1 + Q_2(A_2/A_0)P_2(\cos\theta) + Q_4(A_4/A_0)P_4(\cos\theta)]. \quad (1)$$

TABLE IV. Spins and multipole-mixing ratios derived from angular-correlation measurements in ^{28}Mg . Spins were determined at the 0.1% confidence level.

Transition (MeV)	J_i	J_f	δ^a
1.47 \rightarrow 0	2	0	0
3.86 \rightarrow 1.47	0	2	0
	1	2	$-\infty \leq \delta \leq \infty$
4.02 \rightarrow 1.47	2	2	$ \delta > 11$
	4	2	0 \pm 0.09
4.56 \rightarrow 1.47	2	2	0.035 \pm 0.030
4.88 \rightarrow 1.47	2	2	0.35 \pm 0.06
4.88 \rightarrow 0	2	0	0
5.17 \rightarrow 1.47	2	2	0.62 \pm 0.09
	3	2	0 \pm 0.09
5.17 \rightarrow 4.02	2	4	0 \pm 0.17
	3	4	0.18 \pm 0.09
5.19 \rightarrow 0	1	0	0
5.47 \rightarrow 1.47	2	2	-0.035 \pm 0.123

^a H. J. Rose and D. M. Brink, Rev. Mod. Phys. **39**, 306 (1967).

The experimental values for the coefficients A_2/A_0 and A_4/A_0 are presented in Table III, and the allowed values for spins and multipole-mixing ratios are given in Table IV. Mixing ratios were obtained by combining the results of the two angular-correlation measurements with appropriate statistical weights. Spins were determined at the 0.1% confidence level. A typical plot of χ^2 vs δ and the best fit to the corresponding angular correlation is shown in Fig. 3 for the 4.02-MeV level. When possible, all members of a γ -ray cascade were analyzed simultaneously in order to determine the spin of the initial level.

III. RESULTS

The results for excitation energies, spins, and parities are summarized in Fig. 4. The spin and

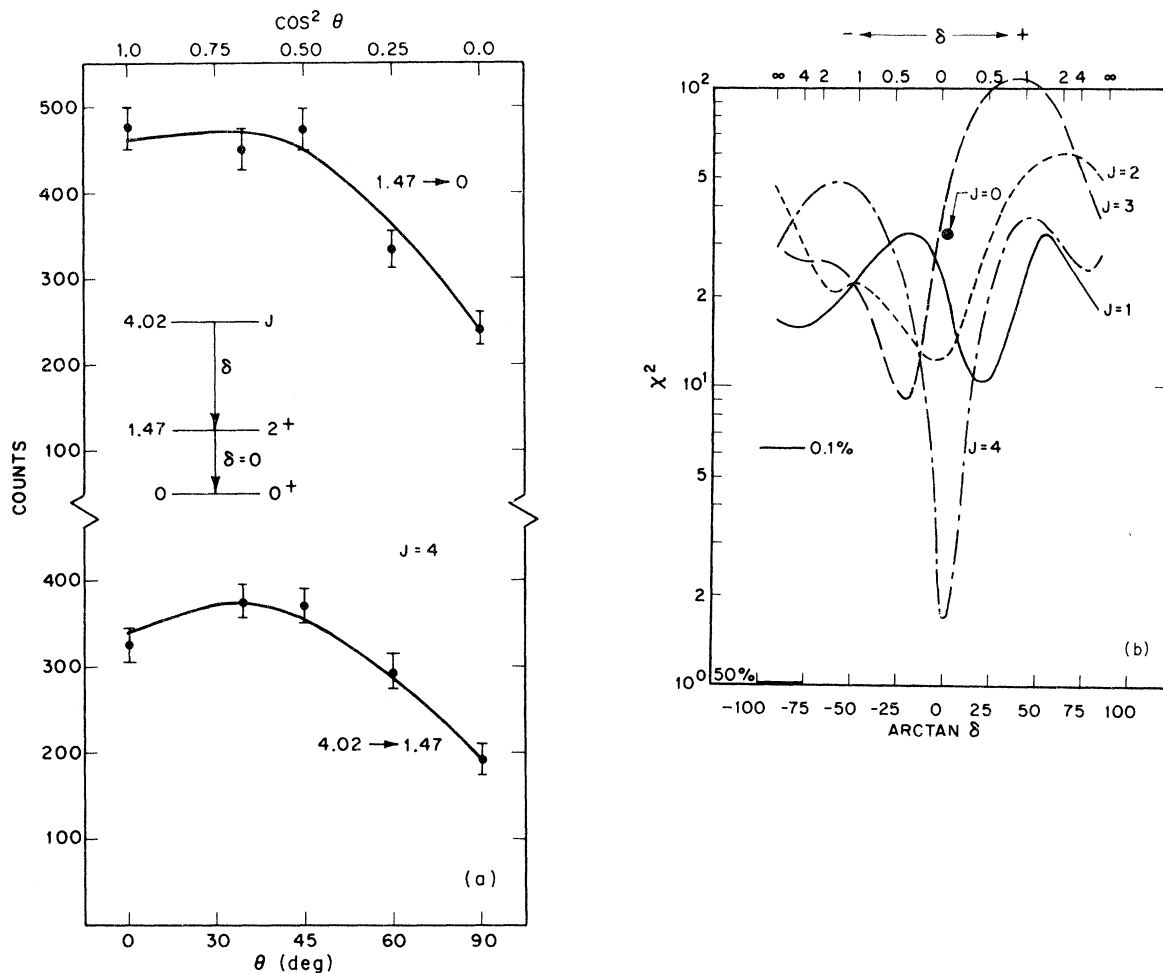


FIG. 3. (a) Experimental γ -ray angular correlations for the 4.02-MeV state. The two cascade γ rays in coincidence with the 4.02-MeV proton group were analyzed simultaneously; the solid curves correspond to a $J=4$ spin assignment ($\delta=0$) for the 4.02-MeV state. (b) χ^2 vs δ plot corresponding to different spin assignments for the 4.02-MeV state. All spin assignments except $J=4$ are eliminated at the 0.1% confidence limit.

parity assignments obtained from analysis of the (t, p) direct reaction data⁴ are shown for comparison, and there is good agreement between the two sets of results. The electromagnetic transition matrix elements derived from these data are presented in Table V.

The spin of the 1.47-MeV level is established as $J=2$ by the angular-correlation data and positive parity is indicated by the lifetime of 1.6 psec [negative parity would imply an $M2$ strength of 450 Weisskopf units (W.u.) for the 1.47 \rightarrow 0 transition]. The angular-correlation data for the 3.86-MeV state are isotropic and are only consistent with a $J=0, 1$, or 2 spin assignment for the 3.86-MeV level. Figures 3(a) and 3(b) show the evidence for a unique $J=4$ assignment for the 4.02-MeV lev-

el. The lifetime of 0.2 psec together with $\delta=0 \pm 0.09$ for the 4.02 \rightarrow 1.47 transition shows that the parity of this level is positive (negative parity would imply an $M2$ strength of 220 W.u. for the transition 4.02 \rightarrow 1.47). A unique $J=2$ assignment is obtained for the levels at 4.56 and 4.88 MeV based on the angular-correlation data. Positive parity is established by the (t, p) double-stripping results.⁴ The transition 4.56 \rightarrow 1.47 is then predominantly $M1$ ($\delta=0.035$), while the 4.88 \rightarrow 1.47 transition is mixed $E2/M1$ ($\delta=0.35 \pm 0.06$).

The assignments of $J^\pi = (3^-)$ and 1^- were obtained in the (t, p) work of Ref. 4 for the levels at 5.17 and 5.19 MeV, respectively. The proton groups from these levels were unresolved except at forward angles, where the data indicated a 1^- assignment for

TABLE V. γ -ray transition strengths in ^{28}Mg . Widths are expressed in W.u.

Transition (MeV)	$J^{\pi}_i \rightarrow J^{\pi}_f$	Branch (%)	δ	τ_m (psec)	$\Gamma(E1)$	$\Gamma(M1)$	$\Gamma(E2)$
1.47 \rightarrow 0	$2^+ \rightarrow 0^+$	100	0	1.60 ± 0.20			14.3 ± 1.8
3.86 \rightarrow 1.47	$0^+ \rightarrow 2^+$	100	0	0.75 ± 0.10			2.7 ± 0.4
4.02 \rightarrow 1.47	$4^+ \rightarrow 2^+$	100	0 ± 0.09	0.21 ± 0.07			7.1 ± 2.4
4.56 \rightarrow 1.47	$2^+ \rightarrow 2^+$	100	0.035 ± 0.030	< 0.04		> 0.027	
4.88 \rightarrow 1.47	$2^+ \rightarrow 2^+$	80 ± 3	0.35 ± 0.06	< 0.18		$> 3.0 \times 10^{-3}$	> 0.012
4.88 \rightarrow 0	$2^+ \rightarrow 0^+$	20 ± 3	0	< 0.18			> 0.065
5.17 \rightarrow 1.47	$3^- \rightarrow 2^+$	64 ± 3	0 ± 0.09	0.10 ± 0.03	$(1.30 \pm 0.4) \times 10^{-3}$		
5.17 \rightarrow 4.02	$3^- \rightarrow 4^+$	36 ± 3	0.18 ± 0.09	0.10 ± 0.03	$(2.36 \pm 0.74) \times 10^{-3}$		
5.19 \rightarrow 0	$1^- \rightarrow 0^+$	100	0	< 0.03	$> 2.5 \times 10^{-4}$		

the 5.19-MeV level. The combined proton angular distribution was adequately explained by a combined $l=1$ and 3 stripping pattern, although an $l=2$ distribution was not excluded for the 5.17-MeV group. The present angular-correlation data require a unique $J=1$ assignment for the 5.19-MeV level and limit the spin of the 5.17-MeV level to $J=2$ or 3. The measured lifetime of the 5.17-MeV level eliminates the $J=2$ assignment which requires a strength of 280 W.u. for the transition 5.17 \rightarrow 4.02. We thus obtain unique assignments $J=3$ and 1 for

the 5.17- and 5.19-MeV levels, respectively, and the (t, p) work of Ref. 4 establishes negative parity for both levels. The observed mixing ratio $\delta=0.18 \pm 0.09$ for the transition 5.17 \rightarrow 4.02 is somewhat inconsistent with a 3^- assignment but the uncertainty in this mixing ratio is large. The reported $J^{\pi}=0^+$ level at 5.26 MeV was weakly excited in the experiment of Ref. 4; the 5.26 \rightarrow 1.47 γ -ray transition in the present experiment was less than 15% of the 5.17 \rightarrow 1.47 γ -ray intensity. Therefore, no γ -ray information was obtained on this state. A unique $J=2$ assignment was found for the 5.47-MeV level, for which no spin assignment has been previously reported. The multipole-mixing ratio for the 5.47 \rightarrow 1.47 transition is $\delta = -0.035 \pm 0.123$.

IV. DISCUSSION

The experimental results of Sec. III have been compared with the predictions of two theoretical models, the triaxial rotor model of Kurath³ and

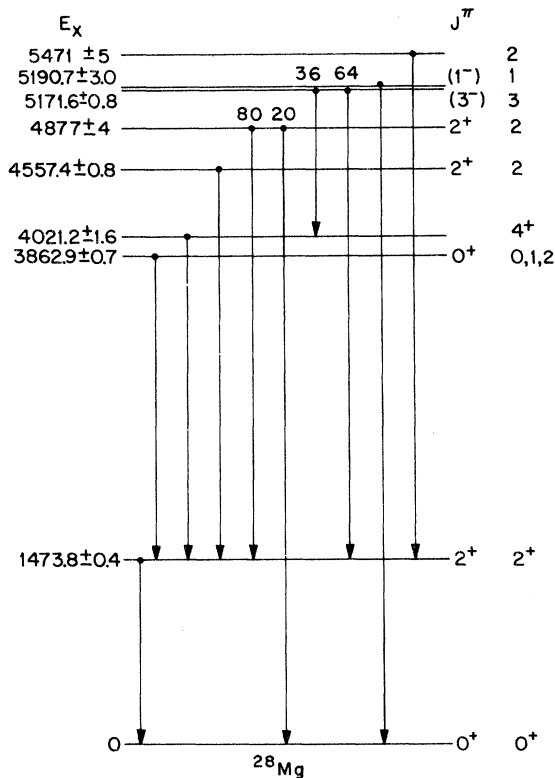


FIG. 4. Level and decay scheme of ^{28}Mg for $E_x < 5.5$ MeV. Values of J^{π} on the left are from Ref. 4; values on the right are from the present work.

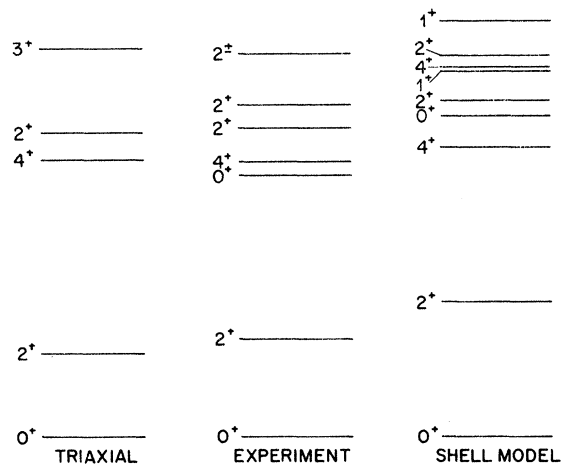


FIG. 5. Comparison between experimental and theoretical level spectra for ^{28}Mg . Results of the triaxial model calculation were furnished by D. Kurath; the shell-model results are from Ref. 7.

the shell-model calculations of de Voigt and Wildenthal.⁷ In the triaxial model calculations, the deformation parameters employed for ³⁰Si and ³²S were retained,³ and the energy-gap parameter which effectively scales the moments of inertia was adjusted to 2 MeV. This changes the energy scale and improves the agreement with the experimental excitation energies with negligible effect on the *E2* transition strengths and energy ratios. In the shell-model calculations, all possible *s-d*-shell configurations were included with the restriction that no more than four holes were allowed in the *d*_{5/2} shell. The parameters of the modified-surface- δ -interaction Hamiltonian were derived by fitting data on ²⁷Al, ²⁸Si, and ²⁹Si, but no ²⁸Mg data were included in these fits. Effective charges $e_p = 1.6e$, $e_n = 0.6e$ were employed in the calculation *E2* matrix elements.

The agreement between the experimental and theoretical level spectra is shown in Fig. 5. The triaxial model does not account for the 0_2^+ and 2_3^+ states which appear in the 4–5-MeV region, and the 3_1^+ state predicted by the model is not seen. However, this level may not be excited in the (*t, p*) reaction, which preferentially excites states having $\pi = (-)^J$. One of the successes of the triaxial model is the correct prediction of the systematic change in the spacing of the 2_1^+ and 2_2^+ levels with *T*. In ²⁴Mg and ³²S (*T*=0) these levels are separated by about 2.5 MeV. In ²⁶Mg and ³⁰Si (*T*=1) the separation has decreased to 1.2 MeV and in ²⁸Mg (*T*=2) the separation is again 2.5 MeV. This systematic feature results naturally from the different occupation of the deformed levels in the triaxial model and requires no adjustment of the deformation parameters. The over-all agreement with the model is similar to that achieved for ²⁶Mg, ³⁰Si, and ³²S. The agreement between the shell-model calculations and experiment is good, considering the fact

that no ²⁸Mg data were used to extract the parameters of the effective Hamiltonian. The 1_1^+ and 4_2^+ levels predicted to occur between 4 and 5.5 MeV were not seen, but the 1^+ level should not be excited by the (*t, p*) reaction and the excitation of the 4_2^+ level may be very weak due to angular momentum considerations. If the 1_1^+ and 4_2^+ levels are omitted, the shell model predicts the correct number of levels below 5.5 MeV excitation although the theoretical energies are consistently high by a few hundred keV.

Electromagnetic transition matrix elements derived from the present data are summarized in Table V, while in Table VI the *E2* and *M1* matrix elements are compared with the theoretical predictions. Of particular interest are the *E2* matrix elements for the $2_1^+ \rightarrow 0_1^+$ and $4_1^+ \rightarrow 2_1^+$ transitions. The triaxial model tends to fix the ratio $B(E2)(4^+ \rightarrow 2^+)/B(E2)(2^+ \rightarrow 0^+)$ close to the value 10/7 (appropriate to *K*=0 states) for both *T*=0 and *T*=1 nuclei. The shell model gives a similar result for the *T*=0 nuclei ²⁴Mg and ³²S, but differs for the *T*=1 nuclei ²⁶Mg and ³⁰Si, where $B(E2)(4^+ \rightarrow 2^+)/(2^+ \rightarrow 0^+) \approx 0.2$; the experimental results for ²⁶Mg and ³⁰Si lie in between the predictions of the two models. ²⁸Mg is the first *T*=2 nucleus for which such a comparison has been made. Reference to Table VI shows that the predictions of the two models are again quite different, with the shell model giving much better agreement with experiment in the ²⁸Mg case.

In summary, the shell-model calculations of de Voigt and Wildenthal give a reasonable account of the present data although the predicted level energies are 500 keV high, on the average. The *B(E2)* values for the $4_1^+ \rightarrow 2_1^+ \rightarrow 0$ transitions are predicted very accurately. The triaxial model gives a good account of the change in spacing of the 2_1^+ and 2_2^+ levels as a function of *T* for the *A*=24–32

TABLE VI. Comparison between theoretical and experimental matrix elements.

Transition ($E_i \rightarrow E_f$) (MeV)	$B(E2) e^2 \text{fm}^4$		Experimental	$B(M1) \mu_N^2$	
	Shell model ^a	Triaxial ^b		Shell model ^a	Experimental
$2_1^+ \rightarrow 0_1^+$ (1.47 \rightarrow 0)	70	50	73.9 \pm 9.0		0
$0_2^+ \rightarrow 2_1^+$ (3.86 \rightarrow 1.47)	25		14.1 \pm 2.0		0
$4_1^+ \rightarrow 2_1^+$ (4.02 \rightarrow 1.47)	27	71	36.4 \pm 14.0		0
$2_2^+ \rightarrow 2_1^+$ (4.56 \rightarrow 1.47)	0.11	4.5	>0.086	0.52	>0.048
$2_2^+ \rightarrow 0_1^+$ (4.56 \rightarrow 0)	3.8	2.5	>0.30		
$2_3^+ \rightarrow 2_1^+$ (4.88 \rightarrow 1.47)	3.6		>0.83	0.38	>0.0057
$2_3^+ \rightarrow 0_1^+$ (4.88 \rightarrow 0)	11		>0.035		

^a From Ref. 7.

^b The numbers in this column were furnished by D. Kurath.

nuclei, including ^{28}Mg . However, its validity is in some doubt for ^{28}Mg because of its qualitatively incorrect prediction for the ratio $B(E2)(4^+ \rightarrow 2^+)/B(E2)(2^+ \rightarrow 0^+)$. A measurement of the quadrupole moment of the 2_1^+ level would be useful, since the predictions of the shell model (0.17 b) and the triaxial model (-0.14 b) have opposite signs, but unfortunately such a measurement is not feasible

with the techniques currently available.

ACKNOWLEDGMENTS

The authors thank D. Kurath for providing them with the results of the triaxial model calculation. We also thank M. J. A. de Voigt and B. H. Wildenthal for making their ^{28}Mg results available prior to publication.

†Work supported by the Lockheed Independent Research Fund.

¹B. H. Wildenthal, J. B. McGroory, and P. W. M. Glaudemans, Phys. Rev. Lett. **26**, 96 (1971).

²J. B. McGroory and B. H. Wildenthal, Phys. Lett. **34B**, 373 (1971).

³D. Kurath, Phys. Rev. C **5**, 768 (1972).

⁴R. Middleton and D. J. Pullen, Nucl. Phys. **51**, 77 (1964).

⁵L. F. Chase, Jr., et al., Bull. Am. Phys. Soc. **12**, 555 (1967); J. A. Becker, in *The Structure of Low-Medium Mass Nuclei*, edited by J. P. Davidson (University Press of Kansas, Lawrence, 1968), pp. 1-22; L. F. Chase, Jr., *Nuclear Research with Low Energy Accelerators* (Academic, New York, 1967), p. 445.

⁶A. E. Litherland and A. J. Ferguson, Can. J. Phys. **39**, 788 (1961).

⁷M. J. A. de Voigt and B. H. Wildenthal, to be published in

Nucl. Phys.

⁸R. A. Chalmers, IEEE Trans. Nucl. Sci. **16**, 132 (1969).

⁹R. K. Bardin, California Institute of Technology Report No. Ba61 (unpublished).

¹⁰J. Lindhard, M. Scharff, and H. E. Schiøtt, K. Dan. Vidensk. Selsk. Mat.-Fys. Medd. **33**, No. 14 (1963).

¹¹A. E. Blaugrund, Nucl. Phys. **88**, 501 (1966).

¹²J. H. Ormrod, J. R. MacDonald, and H. E. Duckworth, Can. Phys. **43**, 275 (1965); B. Fastrup, P. Hvelplund, and C. A. Sautter, K. Dan. Vidensk. Selsk. Mat.-Fys. Medd. **35**, No. 10 (1966).

¹³C. P. Swann, Phys. Rev. C **4**, 1489 (1971); D. Vitoux, R. C. Haight, and J. X. Saladin, Phys. Rev. C **3**, 718 (1971); O. Häusser, B. W. Hooton, D. Pelte, and T. K. Alexander, Can. J. Phys. **48**, 35 (1970); S. J. Skorka, D. Evers, J. Hertel, J. Morgenstern, T. W. Retz-Schmidt, and H. Schmidt, Nucl. Phys. **81**, 370 (1966).

Study of the Energy Levels of ^{69}Ga Using Nuclear Photoexcitation

R. Moreh, O. Shahal, J. Tenenbaum, A. Wolf, and A. Nof

Nuclear Research Center, Negev, Beer Sheva, Israel

(Received 10 October 1972)

Elastic and inelastic scattering of monochromatic photons were used for studying nuclear energy levels in ^{69}Ga ; the photons were produced by thermal neutron capture in copper and vanadium. The decay of one resonance at 7306 keV excited by the copper γ source and another resonance at 6874 keV excited by the vanadium γ source were studied in detail and 30 low-lying levels were observed from the ground state up to 3.4 MeV, 17 of which are believed to be new levels in ^{69}Ga . The angular distribution of some elastic and inelastic lines were measured and the following spin determinations were made (keV, J^π): 320, $\frac{1}{2}^-$, ($\frac{3}{2}^-$); 574, $\frac{5}{2}^-$; 872, $\frac{3}{2}^-$; 1488, $\frac{3}{2}^-$, $\frac{7}{2}^-$; 1525 ($\frac{1}{2}$, $\frac{3}{2}$); 1891, $\frac{3}{2}^-$; (1978), ($\frac{1}{2}$, $\frac{3}{2}$); 2457, $\frac{3}{2}$; 2484, $\frac{5}{2}$; (2565), ($\frac{1}{2}$, $\frac{3}{2}$); 2660, $\frac{3}{2}$; 3051, ($\frac{3}{2}$, $\frac{7}{2}$); 3076, $\frac{5}{2}$; 3318, ($\frac{7}{2}$); 6874, $\frac{1}{2}^{(+)}$ and 7306, $\frac{5}{2}^+$, where parentheses denote uncertain J^π assignments. The parity of the 7306-keV level was directly determined using a Compton polarimeter. The total radiative width of the 7306-keV level was measured and found to be $\Gamma = 0.105 \pm 0.020$ eV. For the 6874-keV level, a positive correlation coefficient was obtained, $\rho = 0.69$, between the (γ, γ') and (d, n) transition strengths leading to the same final states in ^{69}Ga . The levels of ^{69}Ga are compared with recent theoretical calculations.

I. INTRODUCTION

In the past few years, the technique of nuclear photoexcitation using neutron capture γ rays, has been employed for studying the energies and spectroscopic properties of nuclear levels in several

isotopes.¹⁻⁸ In the present work, the same technique is used for studying the energy levels of ^{69}Ga using γ sources obtained from thermal neutron capture in copper and vanadium. The deexcitation of the 7306-keV level of ^{69}Ga excited by the γ rays of copper had been studied in detail.